HHS Public Access

Author manuscript

Circulation. Author manuscript; available in PMC 2016 October 13.

Published in final edited form as:

Circulation. 2015 October 13; 132(15): 1377–1386. doi:10.1161/CIRCULATIONAHA.114.015125.

Small Conductance Calcium-Activated Potassium Current is Activated During Hypokalemia and Masks Short Term Cardiac Memory Induced by Ventricular Pacing

Yi-Hsin Chan, MD[1,2], **Wei-Chung Tsai, MD**[1,3], **Jum-Suk Ko, MD, PhD**[4], **Dechun Yin, MD**[5], **Po-Cheng Chang, MD**[1,2], **Michael Rubart, MD**[6], **James N. Weiss, MD**[7], **Thomas Everett IV, PhD**[1], **Shien-Fong Lin, PhD**[1,8], and **Peng-Sheng Chen, MD**[1]

[1]The Krannert Institute of Cardiology and Division of Cardiology, Department of Medicine, Indiana University School of Medicine, Indianapolis, IN

[2]Division of Cardiology, Department of Internal Medicine, Chang Gung Memorial Hospital, Chang Gung University College of Medicine, Linkou, Taoyuan, Taiwan

[3]Division of Cardiology, Department of Internal Medicine, Kaohsiung Medical University Hospital, Kaohsiung University College of Medicine, Kaohsiung, Taiwan

[4]Division of Cardiology, Department of internal medicine, Wonkwang University School of Medicine and Hospital, Jeonbuk, Republic of Korea

[5]Department of Cardiology, the First Affiliated Hospital of Harbin Medical University, Harbin, China

[6]Wells Center for Pediatrics Research, Department of Pediatrics, Indiana University School of Medicine, Indianapolis, IN

[7]Departments of Medicine (Cardiology) and Physiology, University of California, Los Angeles, CA

[8]Institute of Biomedical Engineering, National Chiao-Tung University, Hsin-Chu, Taiwan

Abstract

Background—Hypokalemia increases the vulnerability to ventricular fibrillation (VF). We hypothesize that the apamin-sensitive small conductance calcium-activated potassium current (I_{KAS}) is activated during hypokalemia and that I_{KAS} blockade is proarrhythmic.

Methods and Results—Optical mapping was performed in 23 Langendorff perfused rabbit ventricles with atrioventricular block and either right ventricular (RV) or left ventricular (LV) pacing during normokalemia or hypokalemia. Apamin prolonged the action potential duration (APD) measured to 80% repolarization (APD_{80}) by 26 ms [95% confidence interval, CI, 14–37] during normokalemia and by 54 ms [CI, 40 to 68] during hypokalemia (P=0.01) at 1000 ms pacing cycle length (PCL). In hypokalemic ventricles, apamin increased the maximal slope of APD restitution, the PCL threshold of APD alternans, the PCL for wavebreak induction and the

Correspondence: Peng-Sheng Chen, MD, The Krannert Institute of Cardiology, Division of Cardiology, Indiana University School of Medicine, 1800 N. Capitol Ave, E475, Indianapolis, IN 46202, Phone: 317-274-0909, Fax: 317-962-0588, chenpp@iu.edu.

Disclosures: Shien-Fong Lin and Peng-Sheng Chen have equity interest in Arrhythmotech, LLC.

area of spatially discordant APD alternans. Apamin significantly facilitated the induction of sustained VF (from 3/9 hearts to 9/9 hearts, P=0.009). Short term cardiac memory was assessed by the slope of APD_{80} versus activation time. The slope increased from 0.01 [CI, −0.09 to 0.12] at baseline to 0.34 [CI, 0.23 to 0.44] after apamin (P<0.001) during RV pacing, and from 0.07 [CI, −0.05 to 0.20] to 0.54 [CI, 0.06 to 1.03] after apamin infusion (P=0.045) during LV pacing. Patch-clamp studies confirmed increased I_{KAS}in isolated rabbit ventricular myocytes during hypokalemia (P=0.038).

Conclusions—Hypokalemia activates I_{KAS} to shorten APD and maintain repolarization reserve at late activation sites during ventricular pacing. I_{KAS} blockade prominently lengthens the APD at late activation sites and facilitates VF induction.

Keywords

action potentials; electrophysiology; pacing; reentry; tachyarrhythmias

Introduction

Hypokalemia is a known risk factor of sudden cardiac death.[1] Hypokalemia promotes ventricular tachyarrhythmias via multiple electrophysiological mechanisms including prolonged ventricular repolarization, slowed conduction, steepened electrical restitution and abnormal pacemaker activity.[2] Hypokalemia directly suppresses several repolarization K^+ currents including the inward rectifier potassium currents (I_{K1}),[3, 4] rapid component of the delayed rectifier potassium currents (I_{Kr})[5, 6] and the transient outward currents (I_{to}).[4] In addition, hypokalemia induces intracellular Ca^{2+} (Ca_i) overload secondary to inhibition of Na^+-K^+ pump and suppression of forward mode Na^+-Ca^{2+} exchanger.[2, 3, 7, 8] The apamin-sensitive small conductance calcium activated K^+ current (I_{KAS}) is known to influence repolarization of normal atria[9, 10] and in failing or infarcted ventricles.[11] In contrast, it is generally believed that I_{KAS} is not important in ventricular repolarization in normal ventricles during normokalemia.[10, 12] By inducing Ca_i overload, hypokalemia might augment the conductance and trafficking of SK channels[13] to upregulate I_{KAS} in normal ventricles. The increased I_{KAS} may help maintain repolarization reserve when other K currents are suppressed by hypokalemia. Blocking I_{KAS} during hypokalemia may be proarrhythmic. Because of the importance of hypokalemia in cardiac arrhythmogenesis, we investigated whether or not I_{KAS} is activated during hypokalemia and, if so, whether I_{KAS}blockade during hypokalemia is proarrhythmic.

Methods

A detailed method section can be found in an Online Supplement.

Optical mapping studies

Surgical preparation—The protocol was approved by the Institutional Animal Care and Use Committee. A total of 23 New Zealand white rabbits were used for optical mapping studies. Among them, 7 were used for normokalemic experiments, 13 for hypokalemic experiments that include 9 with right ventricular (RV) pacing and 4 with left ventricular

(LV) pacing, and 3 for hypokalemia experiments during atrial pacing. The hearts were Langendorff perfused with 37°C oxygenated Tyrode's solution. The composition of Tyrode's solution in normokalemic experiments (N=7) was (in mmol/L): NaCl 128, KCl 4.7, $NaHCO_3$ 24, NaH_2PO_4 1.8, $CaCl_2$ 1.8, $MgCl_2$ 1.2, glucose 11.1 and bovine serum albumin 40 mg/L with a pH of 7.40. In hypokalemic experiments, the KCL was decreased to 2.4 mmol/L once hearts were cannulated. We then performed radiofrequency atrioventricular (AV) node ablation to reduce the ventricular rate.

Optical Mapping—We performed simultaneous optical mapping of the membrane potential (V_m) and Ca_i using techniques similar to that reported elsewhere.[14] The hearts were stained with Rhod-2 AM (Invitrogen, Grand Island, NY) for Ca_imapping and then RH237 (Invitrogen, Grand Island, NY) for V_m mapping. Blebbistatin (Tocris Bioscience, Minneapolis, MN) was used to inhibit contraction. The hearts were excited with a laser (Verdi G5, Coherent Inc., Santa Clara, CA) at a wavelength 532 nm. The signals were recorded simultaneously with two MiCAM Ultima cameras (BrainVision, Tokyo, Japan).

Pseudoelectrocardiogram (pECG) was monitored using 2 electrodes placed in the left atrium and the RV, respectively. The RV was paced at 300 ms pacing cycle length (PCL) throughout the experiment except when interrupted by dynamic pacing or programmed stimulation. A dynamic pacing protocol was performed to determine the action potential duration restitution (APDR) curve. A S1/S2/S3 (short/long/short) pacing protocol and long/short coupled pacing protocol were used to simulate the ECG characteristics that initiates the early afterdepolarizations (EADs) and torsades de pointes (TdP) ventricular tachycardia in humans. Apamin (100 nmol/L) was then added to the perfusate and the ventricles were continuously paced at 300 ms PCL for an hour. The protocols were then repeated. Four additional hearts were studied during hypokalemia with LV pacing. Three additional hearts were paced from the right atrial appendage at 300 ms PCL.

I_{KAS} densities determined by voltage-clamp techniques

Additional rabbit hearts were used for patch clamp studies according to previously described methods.[15] Briefly, isolated ventricular myocytes were used for whole-cell I_{KAS} recording using the voltage-clamp technique in the ruptured-patch configuration.[16] The extracellular solution contained (in mmol/L): N-methylglucamine (NMG) 140, $MgCl_2$ 1, glucose 5, HEPES 10 (pH 7.4 using HCl), and KCl 4.7 or 2.4. The internal solution consisted of (in mmol/L): potassium gluconate 144, $MgCl_2$ 1.15, EGTA 5, HEPES 10, and $CaCl_2$ yielding a free Ca^{2+}-concentration of 1 μmol/L. All experiments were carried out at room temperature. Currents were elicited using a voltage-ramp from +40 to −100 mV (0.35 mV/s) from a holding potential of −50 mV. Voltage-ramps were repeated every 10 s. Once the currents had stabilized, the cell was exposed to the same bath solution supplemented with apamin (100 nmol/L). Currents recorded in the presence of apamin were digitally subtracted from those measured in its absence and the density of the apamin-sensitive current at 0 mV was calculated.

Data Analysis

APD_{80} was measured at the level of 80% repolarization of the action potential. The mean APD_{80} was calculated for all available ventricular pixels. The F/F_0 ratio was used to estimate the relative concentration of Ca_i[17] between normokalemia and hypokalemia and between early and late activation sites. Continuous variables are expressed as mean and 95% confidence interval (CI). We used the term “delta” to indicate the mean on the corresponding difference between two measures (i.e. post minus pre). Paired Student's t-tests were used to compare continuous variables measured at baseline and during apamin infusion. Independent sample t-test was used to compare the I_{KAS} current densities with 4.7 mmol/L and 2.4 mmol/L potassium concentration in the Tyrode solution. Comparison of prevalence of VF inducibility between baseline and during apamin infusion was performed using Fisher’s exact test. A 2-sided $P \leq 0.05$ was considered statistically significant.

Results

Effects of I_{KAS} blockade on rabbit ventricles during hypokalemia

The maximum Ca^{2+} F/F_0 at a LV apex during ventricular pacing at 300 ms PCL was 1.12 [CI, 1.08 to 1.17, N=7] when potassium concentration was 4.7 mmol/L, and increased to 1.29 [CI, 1.23 to 1.35, N=13] when the potassium concentration decreased to 2.4 mmol/L ($P < 0.001$). The F/F_0 was 1.17 [CI, 1.14 to 1.20] at early activation sites and 1.29 [CI, 1.22 to 1.35] (delta=0.12 [CI, 0.07 to 0.17], $P < 0.001$, N=13) at late activation sites, respectively, at baseline and 1.14 [CI, 1.11 to 1.18] and 1.27 [CI, 1.21 to 1.32] for the hypokalemic hearts (delta=0.12 [CI, 0.08 to 0.16], $P < 0.001$, N=13), respectively, after addition of apamin. The latter findings were consistent with Ca_i accumulation at late activation sites during ventricular pacing.[18] Typical examples are shown in the Online Supplement Figure 1.

We tested the effects of apamin on 9 rabbit ventricles with RV pacing during hypokalemia ($[K^+]_0$ = 2.4 mmol/L). Optical images were captured from the whole ventricle. As shown in Figure 1A, apamin prolonged APD_{80} at all PCLs during hypokalemia. However, the effects were more apparent at long than short PCLs (Figures 1B and 1C). At the PCL of 1000 and 250 ms, apamin prolonged the APD_{80} from 215 [CI, 205 to226] to 269 ms [CI, 250 to 289] (delta=54 [CI, 40 to 68], $P < 0.01$) and from 173 [CI, 165 to 180] to 189 ms [CI, 178 to 199], respectively (delta=16 [CI, 10 to 22], $P < 0.01$). The average magnitudes of APD_{80} prolongation at 1000 ms and at 250 ms PCL were 54 ms [CI, 40 to 68] and 16 ms [CI, 10 to 22], respectively. The percentage of prolongation at PCLs of 1000 and 250 ms were 25.38% [CI, 19.24 to 31.52%] and 9.23% [CI, 6.09 to 12.38%], respectively. We also tested the effects of apamin in 7 normokalemic ventricles ($[K^+]$ = 4.7 mmol/L). Apamin had very little effect on APD_{80} at 250 and 300 ms PCL, but increased the APD_{80} by 14% at 1000 ms PCL (from 182 ms [CI, 170 to 194] to 208 ms [CI, 188 to 227]; delta=26 [CI, 14 to 37], P = 0.01). The average magnitude of APD_{80} prolongation at 1000 ms PCL was 26 ms [CI, 14 to 37], which was significantly less than that during hypokalemia (P = 0.01). Online Supplement Figure 2 summarizes the effects of apamin on APD in normokalemic ventricles.

APD heterogeneity has been recognized as an important factor contributing to reentrant ventricular arrhythmia. We used the standard deviation (SD) and correlation of variance

(COV) generated from the optically imaged region to quantify APD heterogeneity. Figure 2A shows APD maps at baseline, after apamin and the ΔAPD maps. Figure 2B shows that apamin significantly increased the SD of APD_{80} at all PCLs. Apamin also significantly increased COV of APD_{80} at 250, 300 and 500 ms PCLs. The changes of COV of at 800 and 1000 ms PCL were insignificant.

Effect of I_{KAS} blockade on the maximal slope of APD Restitution (APDR) in hypokalemic ventricles

APDR curves were sampled at a basal and apical area over the LV in each heart studied. In a representative ventricle (Figure 3A), APDR slope after I_{KAS} inhibition was consistently higher than baseline at both slow (1000 ms) and fast (200 ms) PCL. I_{KAS} blockade also increased the maximal slope of APDR as compared with the baseline in both basal and apical region. For 9 hearts with RV pacing studied, I_{KAS} blockade increased the maximal slope of APDR from 0.99 [CI, 0.81 to 1.17] at baseline to 1.26 [CI, 1.04 to 1.47] (delta=0.26 [CI, 0.14 to 0.39], $P < 0.01$) (Figure 3B).

I_{KAS} blockade facilitated the development of 2:2 alternans and wavebreaks in hypokalemic ventricles

Rapid pacing was associated with a heterogeneous distribution of APD and the calcium transients duration (CaTD) during hypokalemia, but less so during normokalemia (Online Supplement Figure 3). In that example, CaTD alternans developed at 220 ms PCL, while both CaTD and APD alternans were observed at 190 ms PCL during hypokalemia, but no alternans was observed during normokalemia at 190 ms PCL. For all hearts studied, the longest PCL that induced CaTD alternans during hypokalemia was 237 ms [CI, 223 to 250], significantly longer than the longest PCL associated with APD alternans (201 ms, [CI, 189 to 214], delta=36 [CI, 20 to 51], $P < 0.001$).

Rapid pacing caused conduction delay during hypokalemia, which was exacerbated by apamin. For 9 hypokalemic ventricles with RV pacing, apamin increased the total activation time from 26 [CI, 21 to 31] to 36 ms [CI, 28 to 43] at 250 ms PCL (delta=9 [CI, 2 to 16], $P = 0.014$). In addition, rapid pacing causes APD alternans, especially at sites remote from the pacing site (Figure 4A). As shown in Figure 4B, the PCL threshold of alternans was significantly prolonged by apamin (250 ms [CI, 225 to 274] vs 201 ms [CI, 189 to 214] at baseline; delta=49 [CI, 20 to 78], $P < 0.01$). Further decreases in PCL caused wavebreak in 4 ventricles (44.4%) at baseline and in all ventricles (100%) after apamin. The PCL threshold inducing wavebreak was also longer after adding apamin (186 ms [CI, 163 to 208]) than at baseline (160 ms [CI, 147 to 173]; delta=26 [CI, 11 to 40], $P < 0.01$).

APD alternans was initially concordant but became discordant when PCL was shortened. Figure 5 shows examples of discordant alternans induced by rapid pacing at baseline and after apamin. To quantify the degree of spatially discordant APD alternans in each ventricle, we calculated the total pixel numbers showing discordant alternans before and after apamin infusion at the shortest PCL that allowed 1:1 capture. At baseline, 4 ventricles (44.4%) showed small areas of spatially discordant APD alternans at 140 to 200 ms PCL. Apamin facilitated the formation of spatially discordant APD alternans by lengthening the nodal line

and enlarging the area involved in alternans (Figure 5A). For all 9 hypokalemic hearts with RV pacing, apamin significantly increased the area ratio (% mapped region) of spatially discordant APD alternans from 7.89% [CI, −0.46 to 16.23] to 45.3% [CI, 32.86 to 57.81%] at the shortest PCL that allowed 1:1 capture (delta=37.44% [CI, 27.21% to 47.69%], $P < 0.001$) (Figure 5B). Further decreasing the PCL resulted in wavebreak in 4 ventricles at baseline and in all 9 ventricles after apamin.

I_{KAS} blockade and activation-repolarization coupling

Activation-repolarization coupling was assessed by plotting APD_{80} against the activation time (AT) during pacing. The PCL used for these analyses was 300 ms. Representative plots of APD_{80} vs AT in two hearts with different RV pacing sites are shown in Figure 6A and 6B, respectively. The slope of APD-to-AT was flat at baseline. Apamin caused more APD prolongation at late activation sites than early activation sites, leading to increased APD-to-AT slope. There was a negative correlation of ΔAPD_{80} (APD_{80} after apamin minus that at baseline) versus baseline APD_{80}. For all 9 hearts with RV pacing during hypokalemia, apamin increased the APD-to-AT slope from 0.01 [CI, −0.09 to 0.12] to 0.34 [CI, 0.23 to 0.44] (delta=0.32 [CI, 0.19 to 0.45], $P < 0.001$). We measured the APD-to-AT slope in 4 hypokalemic ventricles studied with recordings available at both 30 min and 90 min after apamin administration. The slope of the APD-AT at 30 min and 90 min were 0.30 [CI, 0.25 to 0.35] and 0.32 [CI, 0.19 to 0.45], respectively ($P = 0.98$), indicating stable APD-to-AT relationship (Figure 7).

We also tested the effect of activation-repolarization coupling in 4 additional ventricles paced from the LV base. Representative plot of APD_{80} vs AT in one heart with LV base pacing is shown in Online Supplement Figure 4. For 4 hearts paced from the LV base, apamin increased the slope of APD-to-AT from 0.07 [CI, −0.05 to 0.20] at baseline to 0.54 [CI, 0.06 to 1.03] (delta=0.47 [CI, 0.02 to 0.93], $P = 0.045$).

Effects of apamin in atrially paced hearts

The APD_{80} at 300 ms PCL at baseline was 153 ms [CI, 128 to 178]. Apamin prolonged the APD_{80} to 176 ms [CI, 143 to 208] (delta=23 [CI, 7 to 39], $P = 0.024$). The entire epicardium was activated within 13 ms [CI, 6 to 21] at baseline and 17 ms [CI, 6 to 27] (delta=3 [CI, 0 to 6], $P = 0.038$) after apamin. While apamin increased AT, it did not change the ventricular activation sequence. The APD-to-AT slope in these 3 hearts was 0.98 [CI, −2.61 to 4.58] at baseline and −0.22 [CI, −1.57 to 1.13] after apamin (delta=-1.20 [CI, −4.62 to 2.23], $P = 0.271$). A representative response to apamin is shown in online supplement Figure 5.

Effects of hypokalemia on I_{KAS}current density

We successfully completed patch clamp studies in isolated rabbit ventricular myocytes with the potassium concentration at 4.7 mM (N=3) and 2.4 mM (N=3) in the Tyrode solution. The densities of I_{KAS} were 0.04 pA/pF [CI −0.04 to 0.12] and 2.20 pA/pF [CI 0.33 to 4.06], respectively (delta=2.16 [CI, 0.30 to 4.02], $P = 0.038$). An example of the patch-clamp study is shown in Online Supplement Figure 6.

I_{KAS} blockade increased ventricular vulnerability to fibrillation in hypokalemic ventricles

No spontaneous tachyarrhythmias were observed during the study. Rapid pacing induced VF episodes in 3 of 9 ventricles (33.3%) studied at baseline. VF episodes were successfully induced in all 9 ventricles (100%) after apamin infusion ($P = 0.009$). In all, there were 8 and 43 VF episodes at baseline and after apamin infusion, respectively. Figure 8A shows phase maps indicating phase singularities (black arrows) during VF episodes at baseline and after I_{KAS} blockade in one representative ventricle. I_{KAS} blockade increased the number of phase singularities of VF episodes ($P = 0.001$, Figure 8B). The short/long/short or long/short coupled pacing protocol did not induce any VF episodes at baseline during hypokalemia. However, VF episodes were successfully induced in 7 ventricles (77.8%) by short/long/short or long/short coupled pacing protocol after apamin infusion ($P = 0.002$). Representative recording of optical mapping in one heart revealed that apamin increased the slope of APD-to-AT from −0.04 to 0.49 at PCL 1000 ms as compared to baseline (Online supplement Figure 7A). The premature stimulation (230 ms coupling interval) captured the tissue near pacing site. However, because of the prolongation of APD remote from pacing site, the impulse was blocked half way through the ventricle, leading to reentry and VF (Online supplement Figure 7B).

Discussion

We found that hypokalemia activated I_{KAS} in normal ventricles with AV block. The effect on APD was greater at longer PCL than at shorter PCL. Blockade of I_{KAS} by apamin under these conditions was proarrhythmic, suggesting that I_{KAS} activation plays an important role in protecting ventricular repolarization reserve and in preventing the development of sustained ventricular arrhythmias of the non-failing ventricles. In addition, apamin unmasked a positive correlation between ΔAPD and AT, indicating that pacing-induced cardiac memory is also modulated by I_{KAS}.

Mechanisms of cardiac memory

Cardiac memory is a term coined by Rosenbaum et al[19] to describe a specialized form of remodeling characterized by an altered T wave recorded induced by a preceding period of altered electrical activation.[20] In the heart, short-term memory refers to the effects of pacing history on the APD and should be distinguished from long-term memory related to changes in gene expression causing electrical remodeling.[21] Short term cardiac memory may be mediated by angiotensin activation induced by altered myocardial stretch during pacing.[22] Angiotensin receptor type 1 (AT-1) forms a complex with the transient outward potassium channel Kv4.3 and regulates its gating properties and intracellular localization.[23] Because transient outward current (I_{to}) is important in the generation of cardiac memory,[24, 25] angiotensin activation leads to a loss of epicardial I_{to},[26] an altered apicobasal repolarization gradient and T wave changes.[27] The short term cardiac memory can also be induced in rabbit ventricles by 5-min of ventricular pacing that returned to control in 5 to 10 minutes.[28] However, losartan, an AT-1 blocker, did not influence the expression of memory in that study. The native rabbit ventricular I_{to1} (chiefly $I_{to1,s}$ encoded by Kv1.4) has an unusually long time constant of recovery from inactivation.[29] Thus, I_{to1} is almost completely inactivated and makes a negligible contribution to the AP at a PCL of < 1 s. I_{KAS} acts like

an I_{to} since its conductance tracks the Ca^{2+} transient. It is possible that in the rabbit ventricles paced at 300 ms PCL, I_{KAS} could form the basis of the memory effect rather than I_{to}.

I_{KAS} and cardiac memory

The induction of cardiac memory in rabbit ventricles can be detected from the relationship between APD and AT.[30] During sinus rhythm or atrial pacing, ventricular APD varies inversely with respect to AT. During ventricular pacing, however, the negative correlation is replaced by a positive correlation lasting about 60 min, after which the negative correlation reestablishes itself. Subsequent studies have suggested that ventricular pacing induces cardiac memory through a mechanoelectrical feedback mechanism[31] related to altered sarcomeric Ca^{2+} handling and cytosolic Ca^{2+} accumulation at sites remote from the pacing site.[18] That mechanism could potentially explain our findings if the increased Ca_i at remote sites activates inward currents that prolong APD, but are compensated by activation of I_{KAS} that attenuates APD prolongation. By inhibiting I_{KAS}, apamin unmasks APD prolongation at remote sites, revealing the underlying positive correlation between APD and AT as a reflection of short term cardiac memory. Our data therefore suggest that short term cardiac memory induced by ventricular pacing is strongly modulated by I_{KAS}.

Importance of short term cardiac memory to ventricular arrhythmogenesis

The safety factor of propagation is determined in part by the spatial patterns of repolarization.[32] Propagation from areas with short APD into areas with long APD is associated with a reduced safety factor of propagation, increasing the propensity for conduction block and reentry. Because pacing-induced short term cardiac memory is associated with greater APD prolongation remote from the pacing site than close to the pacing site, the safety factor of propagation is reduced particularly during premature depolarization. Consistent with this hypothesis, we have shown that apamin administration makes it easier for a premature stimulation to induce wavebreaks.

Another form of cardiac memory is the rate- and/or diastolic interval-dependent changes in APDR.[33] This type of memory is dependent on the kinetic properties of multiple different ion channels. A previous study[34] and the present study indicated that I_{KAS} is important in APDR. In computer simulations, adding a potassium memory current to the Luo-Rudy model showed that the accumulation of the memory potassium current played an important role in the progression of the activation patterns of VF over time by progressively shortening the APD.[21] I_{KAS} activation as Ca overload develops during early VF could act in the same way as a memory K current and thus influences the generation and maintenance of VF.[34, 35]

I_{KAS} and the repolarization reserve

Despite significant APD prolongation during moderate hypokalemic ventricles after I_{KAS} inhibition, spontaneous EADs or TdP were not observed. However, in case of associated disease conditions such as heart failure and co-existent atrioventricular block and bradycardia, spontaneous EADs or TdP may occur after apamin.[14] Another possible explanation is that I_{Ks} and I_{Kr} are activated during the phase 3 of the action potential, while I_{KAS} is most important during the phase 2 of the action potential when $I_{Ca,L}$ activity,

sarcoplasmic Ca^{2+} release and the $Ca_i$are high. The effects of I_{KAS} blockade may be sufficient to prolong the APD. However, without other associated ionic current changes, APD prolongation by itself is insufficient to induce EADs or TdP.[36]

I_{KAS} blockade increases tissue vulnerability in hypokalemic ventricles

We observed increased APD heterogeneity, steepened maximal slope of APDR, increased PCL threshold for alternans and increased spatially discordant APD alternans after I_{KAS} inhibition, factors which increase vulnerability to ventricular arrhythmias.[33, 37, 38] The out-of-phase regions of discordant APD alternans are separated by a nodal line,[39] in which the spatial gradients in APD or Ca_i transient amplitude are the steepest, predisposing to localized conduction block.[33, 40] The augmentation of spatially discordant APD alternans by I_{KAS} blockade in our study can be explained by two mechanisms: I_{KAS} blockade steepened APDR curve in hypokalemic ventricles, which would facilitate the formation of discordant APD alternans.[33] In addition, because V_m and Ca_i are bidirectionally coupled in myocardial tissue, I_{KAS} may play an important role to modulate the V_m and Ca_i coupling. Longer Ca_i transient results in greater I_{KAS} activation to compensate for the longer APD caused by longer Ca_i transient. Therefore, I_{KAS} inhibition would amplify the effect of Ca^{2+} on APD prolongation and hence prolong the PCL threshold for alternans.

Study limitations

The optical mapping techniques do not allow us to determine the absolute levels of the Ca_i. Therefore, we relied on the reports by others to support the altered Ca_i handling at late activated regions.[18] We showed that I_{KAS} blockade facilitated ventricular arrhythmias in hypokalemic normal ventricles, a finding opposite to that in failing ventricles where apamin was anti-fibrillatory.[34] The mechanisms of the opposite observations may be related to additional remodeling changes that are present in failing but not normal ventricles. Apamin has been reported to also block the fetal type $I_{Ca,L}$,[41] implying that it is not a specific ion channel blocker. However, Yu et al[16] recently showed that apamin is a highly specific I_{KAS} blocker for human type cardiac ion channels and does not block $I_{Ca,L.}$

Summary and clinical significance

A large study involving 58,167 hospital inpatients showed that 5.2% had serum potassium less than 3.0 mmol/l, including 73 patients with potassium < 2.0 mmol/L and 472 patients with potassium between 2.0 and 2.4 mmol/L.[42] Hypokalemia significantly increases mortality in hospitalized patients.[42] We showed that I_{KAS} blockade increased the vulnerability to ventricular tachyarrhythmias in hypokalemic ventricles. I_{KAS} also plays an important role in modulating cardiac memory. These findings indicate that I_{KAS} is important in ventricular arrhythmogenesis during hypokalemia. This may be relevant to drug safety, since a number of commonly used clinical drugs are known inhibitors of I_{KAS}, such as anesthetic agents,[43] quinine, *d*-tubocurarine[44] and amiodarone.[45] It is possible that further investigations will discover the I_{KAS} blocking action of other drugs used commonly in clinical practice. The I_{KAS} blocking action may contribute to their proarrhythmic mechanism. Better understanding the drug effects on I_{KAS} may be important in the prevention of sudden death and promote drug safety in patients with severe hypokalemia.

Supplementary Material

Refer to Web version on PubMed Central for supplementary material.

Acknowledgement

We thank Nicole Courtney, Christopher Corr, David Adams and David Wagner for their assistance.

Funding Sources: This work was supported by NIH Grants P01 HL78931, R01 HL71140, R41HL124741, a Medtronic-Zipes Endowment of the Indiana University and the Indiana University Health-Indiana University School of Medicine Strategic Research Initiative.

Our laboratory receives equipment donations from Medtronic, St Jude and Cyberonics Inc.

References

1. Zipes DP, Wellens HJ. Sudden cardiac death. Circulation. 1998; 98:2334–2351. [PubMed: 9826323]
2. Osadchii OE. Mechanisms of hypokalemia-induced ventricular arrhythmogenicity. Fundam Clin Pharmacol. 2010; 24:547–559. [PubMed: 20584206]
3. Bouchard R, Clark RB, Juhasz AE, Giles WR. Changes in extracellular K+ concentration modulate contractility of rat and rabbit cardiac myocytes via the inward rectifier K+ current IK1. J Physiol. 2004; 556:773–790. [PubMed: 14990678]
4. Killeen MJ, Gurung IS, Thomas G, Stokoe KS, Grace AA, Huang CL. Separation of early afterdepolarizations from arrhythmogenic substrate in the isolated perfused hypokalaemic murine heart through modifiers of calcium homeostasis. Acta Physiol (Oxf). 2007; 191:43–58. [PubMed: 17524066]
5. Yang T, Snyders DJ, Roden DM. Rapid inactivation determines the rectification and [K+]o dependence of the rapid component of the delayed rectifier K+ current in cardiac cells. Circ Res. 1997; 80:782–789. [PubMed: 9168780]
6. Guo J, Massaeli H, Xu J, Jia Z, Wigle JT, Mesaeli N, Zhang S. Extracellular K+ concentration controls cell surface density of IKr in rabbit hearts and of the herg channel in human cell lines. J Clin Invest. 2009; 119:2745–2757. [PubMed: 19726881]
7. Weiss JN. Palpitations, potassium and the pump. J Physiol. 2015; 593:1387–1388. [PubMed: 25772294]
8. Aronsen JM, Skogestad J, Lewalle A, Louch WE, Hougen K, Stokke MK, Swift F, Niederer S, Smith NP, Sejersted OM, Sjaastad I. Hypokalaemia induces Ca(2+) overload and Ca(2+) waves in ventricular myocytes by reducing Na(+), K(+) -ATPase α2 activity. J Physiol. 2015; 593:1509–1521. [PubMed: 25772299]
9. Tuteja D, Xu D, Timofeyev V, Lu L, Sharma D, Zhang Z, Xu Y, Nie L, Vazquez AE, Young JN, Glatter KA, Chiamvimonvat N. Differential expression of small-conductance Ca2+-activated K+ channels SK1, SK2, and SK3 in mouse atrial and ventricular myocytes. Am J Physiol Heart Circ Physiol. 2005; 289:H2714–H2723. [PubMed: 16055520]
10. Xu Y, Tuteja D, Zhang Z, Xu D, Zhang Y, Rodriguez J, Nie L, Tuxson HR, Young JN, Glatter KA, Vazquez AE, Yamoah EN, Chiamvimonvat N. Molecular identification and functional roles of a Ca(2+)-activated K+ channel in human and mouse hearts. J Biol Chem. 2003; 278:49085–49094. [PubMed: 13679367]
11. Chang P-C, Chen P-S. SK channels and ventricular arrhythmias in heart failure. Trends Cardiovasc Med. 2015 Jan 29. pii: S1050-1738(15)00031-6. [Epub ahead of print].
12. Nagy N, Szuts V, Horvath Z, Seprenyi G, Farkas AS, Acsai K, Prorok J, Bitay M, Kun A, Pataricza J, Papp JG, Nanasi PP, Varro A, Toth A. Does small-conductance calcium-activated potassium channel contribute to cardiac repolarization? J Mol Cell Cardiol. 2009; 47:656–663. [PubMed: 19632238]
13. Rafizadeh S, Zhang Z, Woltz RL, Kim HJ, Myers RE, Lu L, Tuteja D, Singapuri A, Bigdeli AA, Harchache SB, Knowlton AA, Yarov-Yarovoy V, Yamoah EN, Chiamvimonvat N. Functional interaction with filamin a and intracellular Ca2+ enhance the surface membrane expression of a

small-conductance Ca2+-activated K+ (SK2) channel. Proc Natl Acad Sci U S A. 2014; 111:9989–9994. [PubMed: 24951510]

14. Chang PC, Hsieh YC, Hsueh CH, Weiss JN, Lin SF, Chen PS. Apamin induces early afterdepolarizations and torsades de pointes ventricular arrhythmia from failing rabbit ventricles exhibiting secondary rises in intracellular calcium. Heart Rhythm. 2013; 10:1516–1524. [PubMed: 23835258]
15. Ahmmed GU, Xu Y, Hong Dong P, Zhang Z, Eiserich J, Chiamvimonvat N. Nitric oxide modulates cardiac Na(+) channel via protein kinase A and protein kinase G. Circ Res. 2001; 89:1005–1013. [PubMed: 11717157]
16. Yu CC, Ai T, Weiss JN, Chen PS. Apamin does not inhibit human cardiac Na+ current, L-type Ca2+ current or other major K+ currents. PLoS One. 2014; 9:e96691. [PubMed: 24798465]
17. Tsai CT, Wang DL, Chen WP, Hwang JJ, Hsieh CS, Hsu KL, Tseng CD, Lai LP, Tseng YZ, Chiang FT, Lin JL. Angiotensin II increases expression of α1C subunit of L-type calcium channel through a reactive oxygen species and camp response element-binding protein-dependent pathway in HL-1 myocytes. Circ Res. 2007; 100:1476–1485. [PubMed: 17463319]
18. Jeyaraj D, Wan X, Ficker E, Stelzer JE, Deschenes I, Liu H, Wilson LD, Decker KF, Said TH, Jain MK, Rudy Y, Rosenbaum DS. Ionic bases for electrical remodeling of the canine cardiac ventricle. Am J Physiol Heart Circ Physiol. 2013; 305:H410–H419. [PubMed: 23709598]
19. Rosenbaum MB, Blanco HH, Elizari MV, Lazzari JO, Davidenko JM. Electrotonic modulation of the T wave and cardiac memory. Am J Cardiol. 1982; 50:213–222. [PubMed: 7102553]
20. Patberg KW, Shvilkin A, Plotnikov AN, Chandra P, Josephson ME, Rosen MR. Cardiac memory: Mechanisms and clinical implications. Heart Rhythm. 2005; 2:1376–1382. [PubMed: 16360096]
21. Baher A, Qu Z, Hayatdavoudi A, Lamp ST, Yang MJ, Xie F, Turner S, Garfinkel A, Weiss JN. Short-term cardiac memory and mother rotor fibrillation. Am J Physiol Heart Circ Physiol. 2007; 292:H180–H189. [PubMed: 16891403]
22. Ozgen N, Rosen MR. Cardiac memory: A work in progress. Heart Rhythm. 2009; 6:564–570. [PubMed: 19324320]
23. Doronin SV, Potapova IA, Lu Z, Cohen IS. Angiotensin receptor type 1 forms a complex with the transient outward potassium channel Kv4.3 and regulates its gating properties and intracellular localization. J Biol Chem. 2004; 279:48231–48237. [PubMed: 15342638]
24. Ricard P, Danilo P Jr, Cohen IS, Burkhoff D, Rosen MR. A role for the renin-angiotensin system in the evolution of cardiac memory. J Cardiovasc Electrophysiol. 1999; 10:545–551. [PubMed: 10355696]
25. del Balzo U, Rosen MR. T wave changes persisting after ventricular pacing in canine heart are altered by 4-aminopyridine but not by lidocaine. Implications with respect to phenomenon of cardiac 'memory'. Circulation. 1992; 85:1464–1472. [PubMed: 1555287]
26. Yu H, Gao J, Wang H, Wymore R, Steinberg S, McKinnon D, Rosen MR, Cohen IS. Effects of the renin-angiotensin system on the current I(to) in epicardial and endocardial ventricular myocytes from the canine heart. Circ Res. 2000; 86:1062–1068. [PubMed: 10827136]
27. Janse MJ, Sosunov EA, Coronel R, Opthof T, Anyukhovsky EP, de Bakker JM, Plotnikov AN, Shlapakova IN, Danilo P Jr, Tijssen JG, Rosen MR. Repolarization gradients in the canine left ventricle before and after induction of short-term cardiac memory. Circulation. 2005; 112:1711–1718. [PubMed: 16157774]
28. Sosunov EA, Anyukhovsky EP, Rosen MR. Altered ventricular stretch contributes to initiation of cardiac memory. Heart Rhythm. 2008; 5:106–113. [PubMed: 18055271]
29. Zhao Z, Xie Y, Wen H, Xiao D, Allen C, Fefelova N, Dun W, Boyden PA, Qu Z, Xie LH. Role of the transient outward potassium current in the genesis of early afterdepolarizations in cardiac cells. Cardiovasc Res. 2012; 95:308–316. [PubMed: 22660482]
30. Costard-Jackle A, Goetsch B, Antz M, Franz MR. Slow and long-lasting modulation of myocardial repolarization produced by ectopic activation in isolated rabbit hearts. Evidence for cardiac "memory". Circulation. 1989; 80:1412–1420. [PubMed: 2805275]
31. Jeyaraj D, Wilson LD, Zhong J, Flask C, Saffitz JE, Deschenes I, Yu X, Rosenbaum DS. Mechanoelectrical feedback as novel mechanism of cardiac electrical remodeling. Circulation. 2007; 115:3145–3155. [PubMed: 17562957]

32. Spach MS, Dolber PC, Heidlage JF. Interaction of inhomogeneities of repolarization with anisotropic propagation in dog atria. A mechanism for both preventing and initiating reentry. Circ Res. 1989; 65:1612–1631. [PubMed: 2582593]
33. Weiss JN, Karma A, Shiferaw Y, Chen PS, Garfinkel A, Qu Z. From pulsus to pulseless: The saga of cardiac alternans. Circ.Res. 2006; 98:1244–1253. [PubMed: 16728670]
34. Hsieh YC, Chang PC, Hsueh CH, Lee YS, Shen C, Weiss JN, Chen Z, Ai T, Lin SF, Chen PS. Apamin-sensitive potassium current modulates action potential duration restitution and arrhythmogenesis of failing rabbit ventricles. Circ Arrhythm Electrophysiol. 2013; 6:410–418. [PubMed: 23420832]
35. Chua SK, Chang PC, Maruyama M, Turker I, Shinohara T, Shen MJ, Chen Z, Shen C, Rubart-von der Lohe M, Lopshire JC, Ogawa M, Weiss JN, Lin SF, Ai T, Chen PS. Small-conductance calcium-activated potassium channel and recurrent ventricular fibrillation in failing rabbit ventricles. Circ Res. 2011; 108:971–979. [PubMed: 21350217]
36. Hondeghem LM, Dujardin K, De Clerck F. Phase 2 prolongation, in the absence of instability and triangulation, antagonizes class III proarrhythmia. Cardiovasc Res. 2001; 50:345–353. [PubMed: 11334838]
37. Riccio ML, Koller ML, Gilmour RF Jr. Electrical restitution and spatiotemporal organization during ventricular fibrillation. Circ Res. 1999; 84:955–963. [PubMed: 10222343]
38. Fenton F, Karma A. Vortex dynamics in three-dimensional continuous myocardium with fiber rotation: Filament instability and fibrillation. Chaos. 1998; 8:20–47. [PubMed: 12779708]
39. Hayashi H, Shiferaw Y, Sato D, Nihei M, Lin SF, Chen PS, Garfinkel A, Weiss J, Qu Z. Dynamic origin of spatially discordant alternans in cardiac tissue. Biophys J. 2006; 92:448–460. [PubMed: 17071663]
40. Weiss JN, Qu Z, Chen PS, Lin SF, Karagueuzian HS, Hayashi H, Garfinkel A, Karma A. The dynamics of cardiac fibrillation. Circulation. 2005; 112:1232–1240. [PubMed: 16116073]
41. Bkaily G, Sculptoreanu A, Jacques D, Economos D, Menard D. Apamin, a highly potent fetal L-type Ca2+ current blocker in single heart cells. Am J Physiol. 1992; 262:H463–H471. [PubMed: 1539705]
42. Paice BJ, Paterson KR, Onyanga-Omara F, Donnelly T, Gray JM, Lawson DH. Record linkage study of hypokalaemia in hospitalized patients. Postgrad Med J. 1986; 62:187–191. [PubMed: 3714603]
43. Dreixler JC, Jenkins A, Cao YJ, Roizen JD, Houamed KM. Patch-clamp analysis of anesthetic interactions with recombinant SK2 subtype neuronal calcium-activated potassium channels. Anesth Analg. 2000; 90:727–732. [PubMed: 10702465]
44. Yamamoto T, Kakehata S, Yamada T, Saito T, Saito H, Akaike N. Effects of potassium channel blockers on the acetylcholine-induced currents in dissociated outer hair cells of guinea pig cochlea. Neurosci Lett. 1997; 236:79–82. [PubMed: 9404816]
45. Turker I, Yu C-C, Chang P, Chen Z, Sohma Y, Lin S-F, Chen P-S, Ai T. Amiodarone inhibits apamin-sensitive potassium currents. PLoS One. 2013; 8:e70450. [PubMed: 23922993]

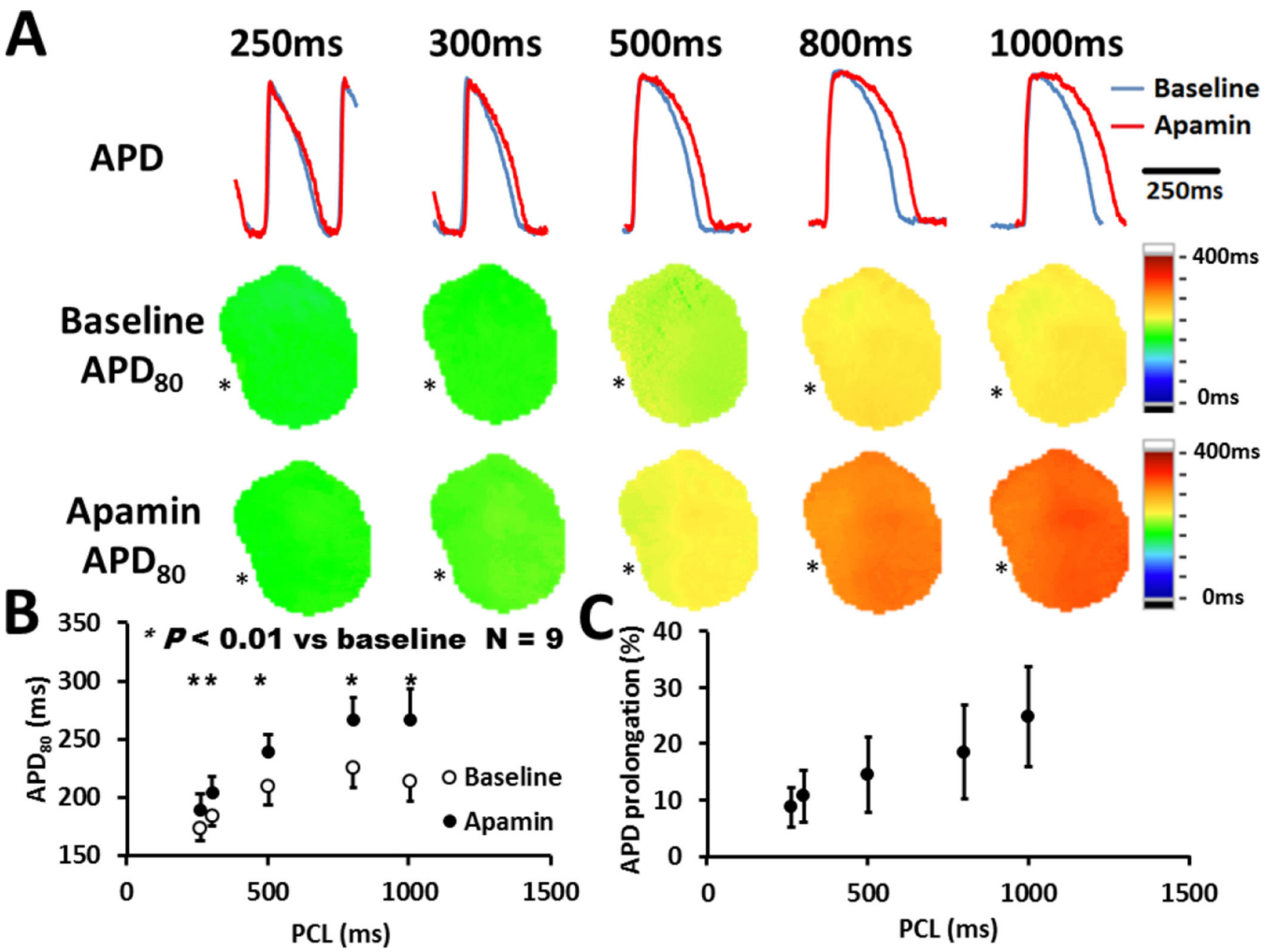

Figure 1.

Effects of I_{KAS} blockade on APD at different PCLs in hypokalemic ventricles. **A**, Representative V_m traces and APD_{80} maps at baseline and in the presence of apamin (100 nmol/L). The magnitude of APD prolongation was more prominent at long PCLs than at short PCLs. An asterisk marks the pacing site. **B**, Apamin significantly prolonged APD_{80} at all PCLs, and the prolongation was more prominent at longer PCLs. *$P < 0.01$. **C**, A plot of ΔAPD_{80} ratio [(APD_{80} after apamin - APD_{80} at baseline)/APD_{80} at baseline] vs PCL shows that apamin prolonged APD_{80} by approximately 25% at a PCL of 1000 ms but only by 9% at a PCL of 250 ms. APD = action potential duration; PCL = pacing cycle length.

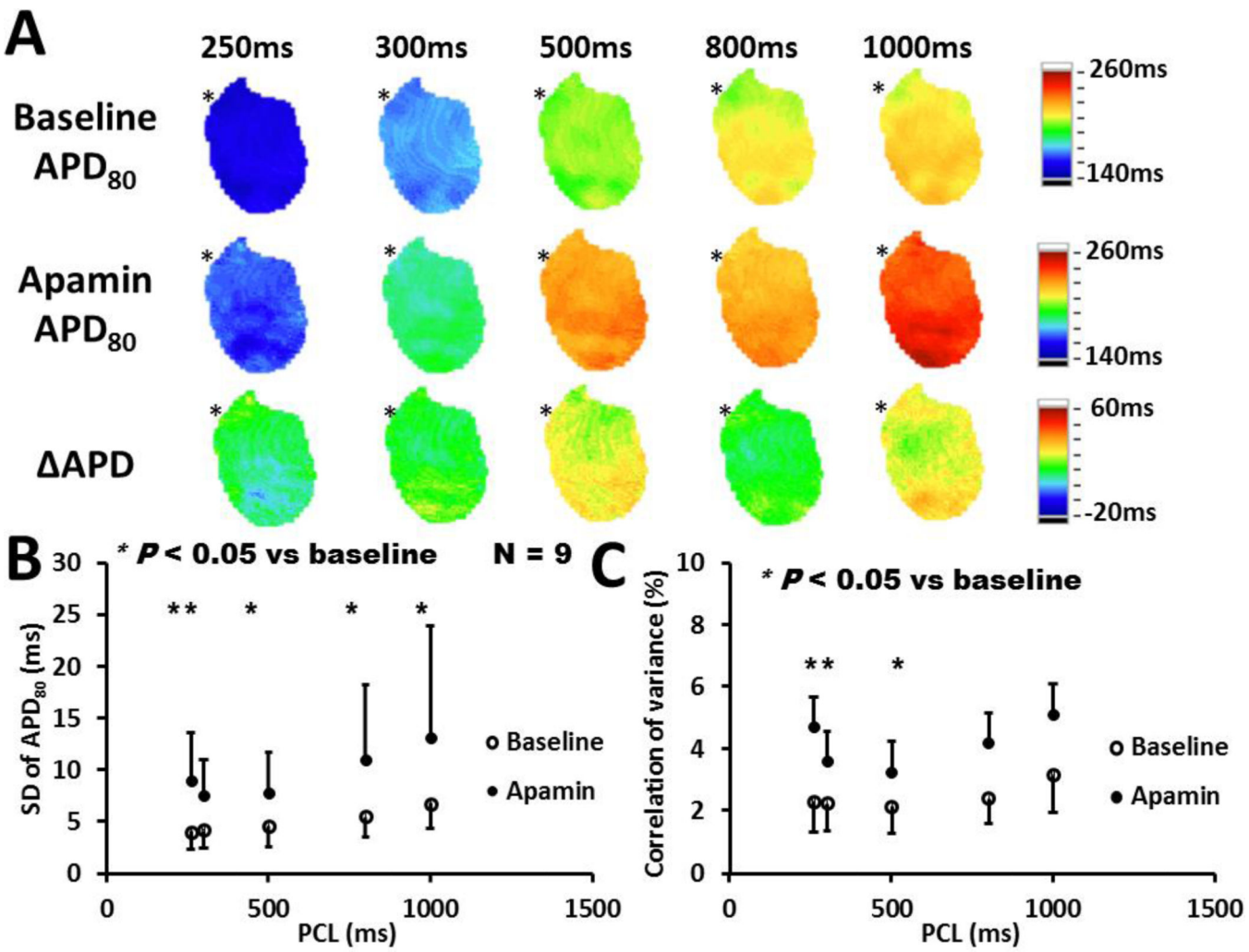

Figure 2.

Effects of I_{KAS} blockade on APD_{80} heterogeneity at different PCLs in hypokalemic ventricles. **A**, Representative APD_{80} maps at baseline (**upper panel**), in the presence of apamin (100 nmol/L) (**middle panel**) and the ΔAPD map (**Lower panel**) at corresponding PCL. The pacing site (asterisk) was located at RV base. **B**, Apamin significantly increased the standard deviation (SD) of APD_{80} at all PCLs, and the prolongation was more prominent at longer PCLs. *$P < 0.05$. **C**, Apamin significantly increased the correlation of variance (COV) of APD_{80} at PCL with 250, 300 and 500 ms, respectively. ΔAPD = APD_{80} after apamin - APD_{80} at baseline. *$P < 0.05$.

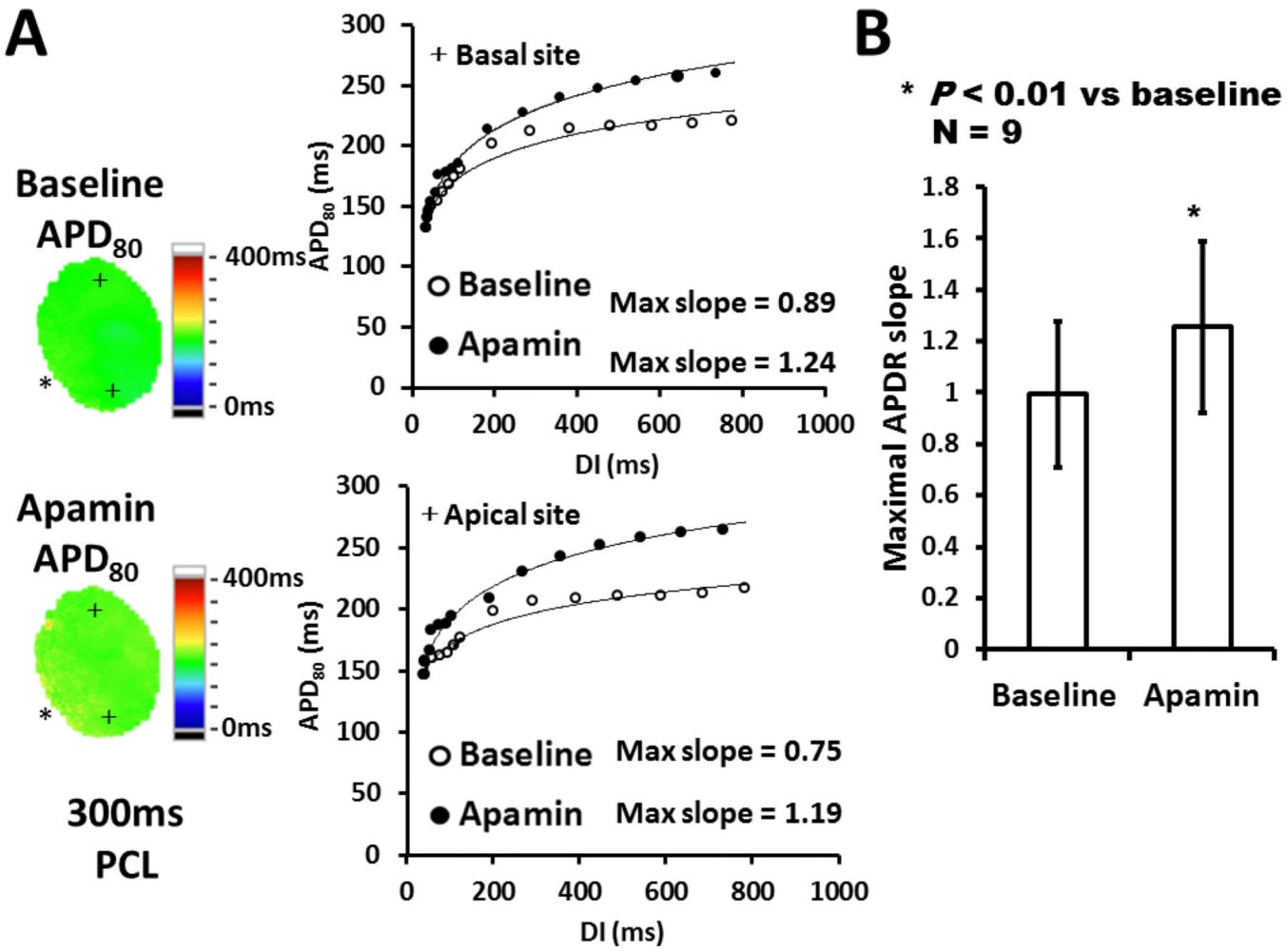

Figure 3.

Effects of I_{KAS} blockade on the maximal slope of APDR curve in hypokalemic ventricles. **A**, APDR curves and maximal slopes of the curves sampled at basal and apical area of one representative ventricle. The pacing site (asterisk) was located at RV apex. **B**, Effects of apamin on the maximal slopes of APDR in normal ventricles during hypokalemia. Apamin significant increased the maximal slope of APDR curve. APDR = action potential duration restitution; I_{KAS} = apamin sensitive small conductance calcium activated potassium current. *$P < 0.01$.

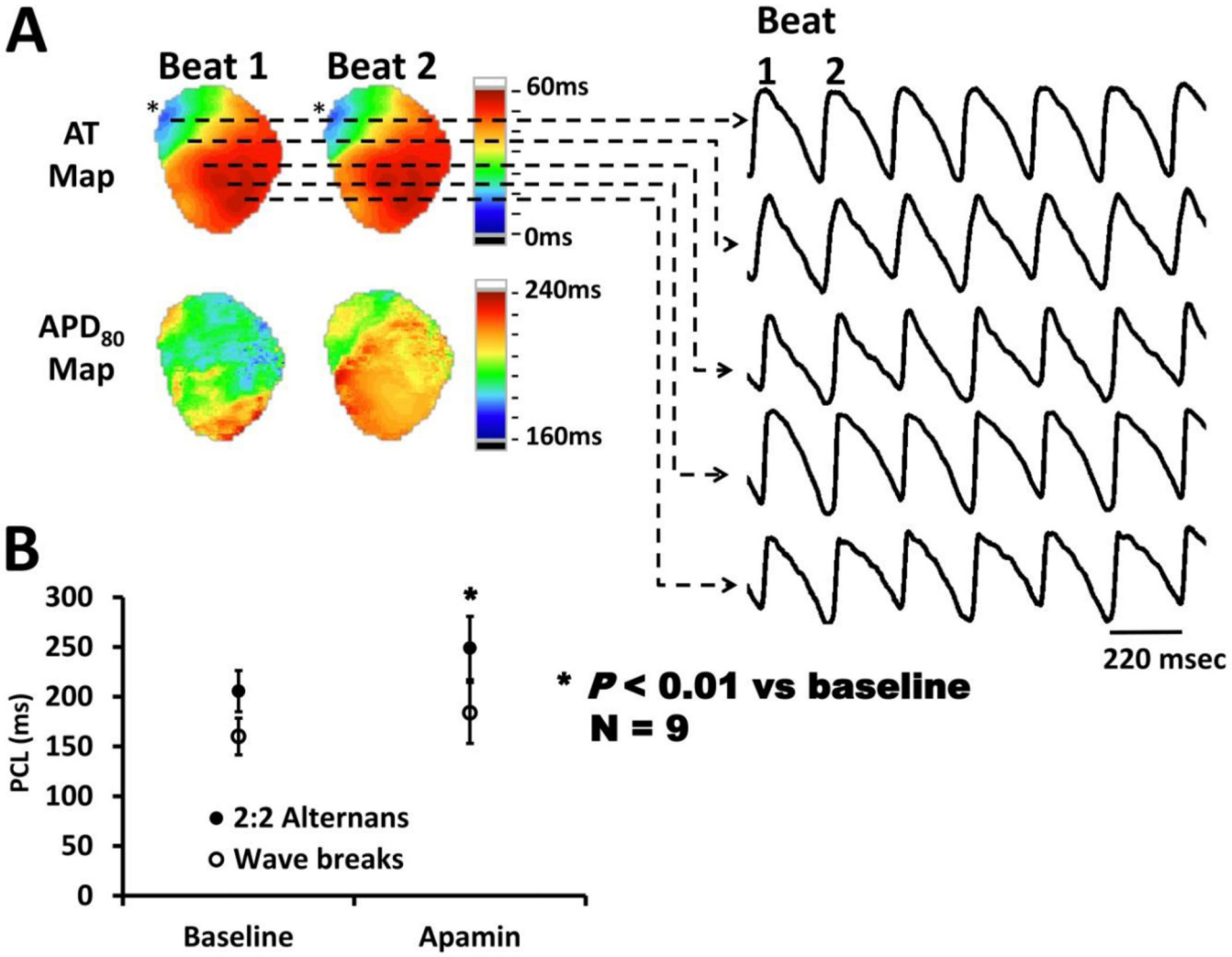

Figure 4.

Development of 2:2 alternans and wavebreaks after I_{KAS} blockade. **A**, Representative trace of 2:2 alternans in one representative hypokalemic ventricle after apamin infusion. Corresponding AT and APD maps from beat 1 and beat 2 are shown. Note there is an obvious 2:2 alternans at the remote activation site. The pacing site is located at RV base (asterisk). **B**, Apamin prolonged the PCL threshold of 2:2 alternans and wavebreaks. Wavebreaks could only be induced in 4 ventricles (44.4%). After I_{KAS} blockade, 9 ventricles (100%) developed 2:2 alternans and all showed wavebreaks at shorter PCLs. APD = action potential duration; AT = activation time; I_{KAS} = apamin sensitive small conductance calcium activated potassium current; PCL = pacing cycle length. RV = right ventricle. *$P < 0.01$.

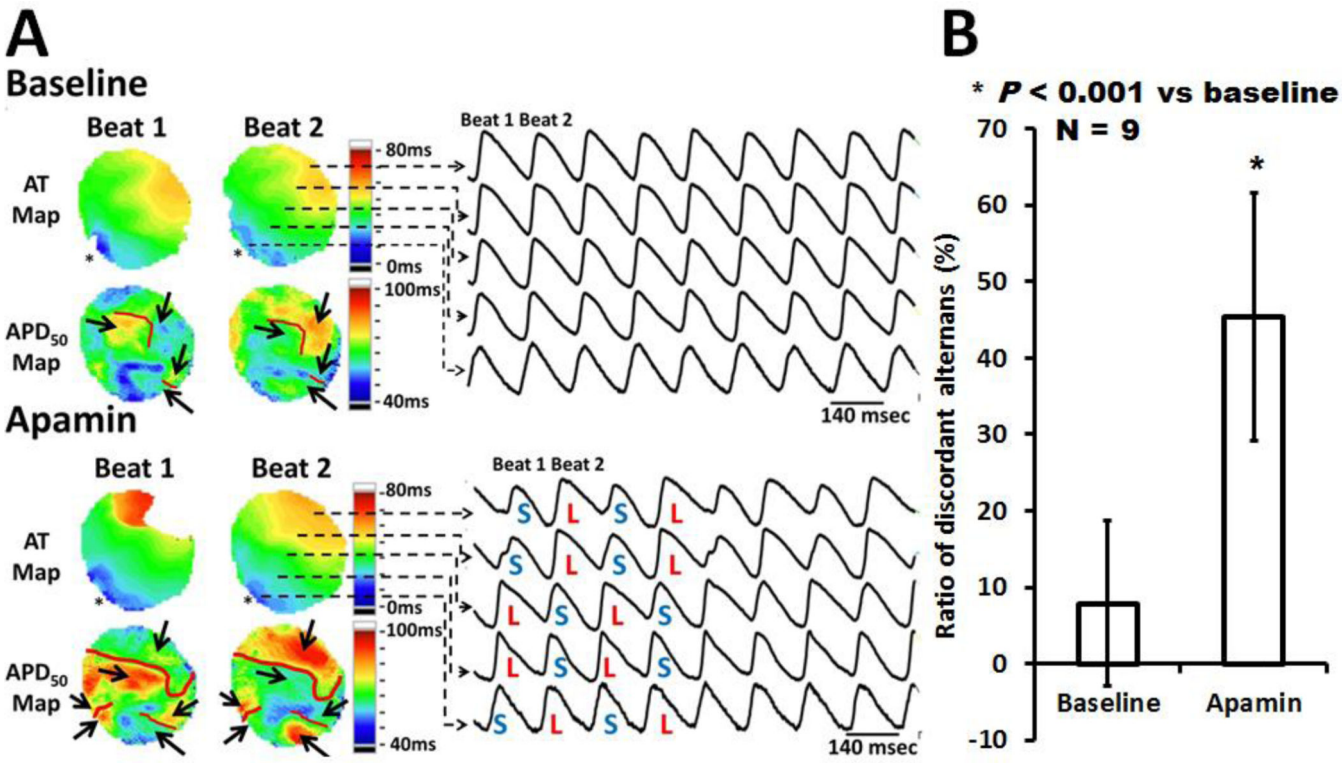

Figure 5.

Development of spatially discordant APD alternans in hypokalemic ventricles after I_{KAS} blockade. **A, Upper**, Corresponding AT and APD maps from beat 1 and beat 2 at baseline with 140 ms PCL, respectively. There were some small areas showing spatially discordant APD alternans within the whole optical area (as arrowheads). Red line indicated the nodal line. The 5 APD tracings sampled from the pacing site to remote site consecutively showed no obvious discordant APD alternans (as arrowheads). **Lower**, Corresponding AT and APD maps from beat 1 and beat 2 are shown after apamin under the same PCL. Note that the area of discordant APD alternans was increased as compared to baseline (as arrows). Red line indicated the nodal line. It is noted that the 5 APD tracings sampled from the pacing site to remote site consecutively showed discordant APD alternans after apamin infusion (as arrowheads). There was wavebreak formation followed by VF when the PCL was further decreased to 140 ms. The pacing site (asterisk) was located at RV apex. **B**, Effects of I_{KAS} blockade on the formation of spatially discordant APD alternans in all hypokalemic ventricles (N = 9). I_{KAS} blockade significantly increased the area ratio of discordant APD alternans to whole optical areas as compared to baseline. APD = action potential duration; AT = activation time; I_{KAS} = apamin sensitive small conductance calcium activated potassium current; L = long APD; PCL = pacing cycle length; RV = right ventricle; S = short APD. *$P < 0.001$.

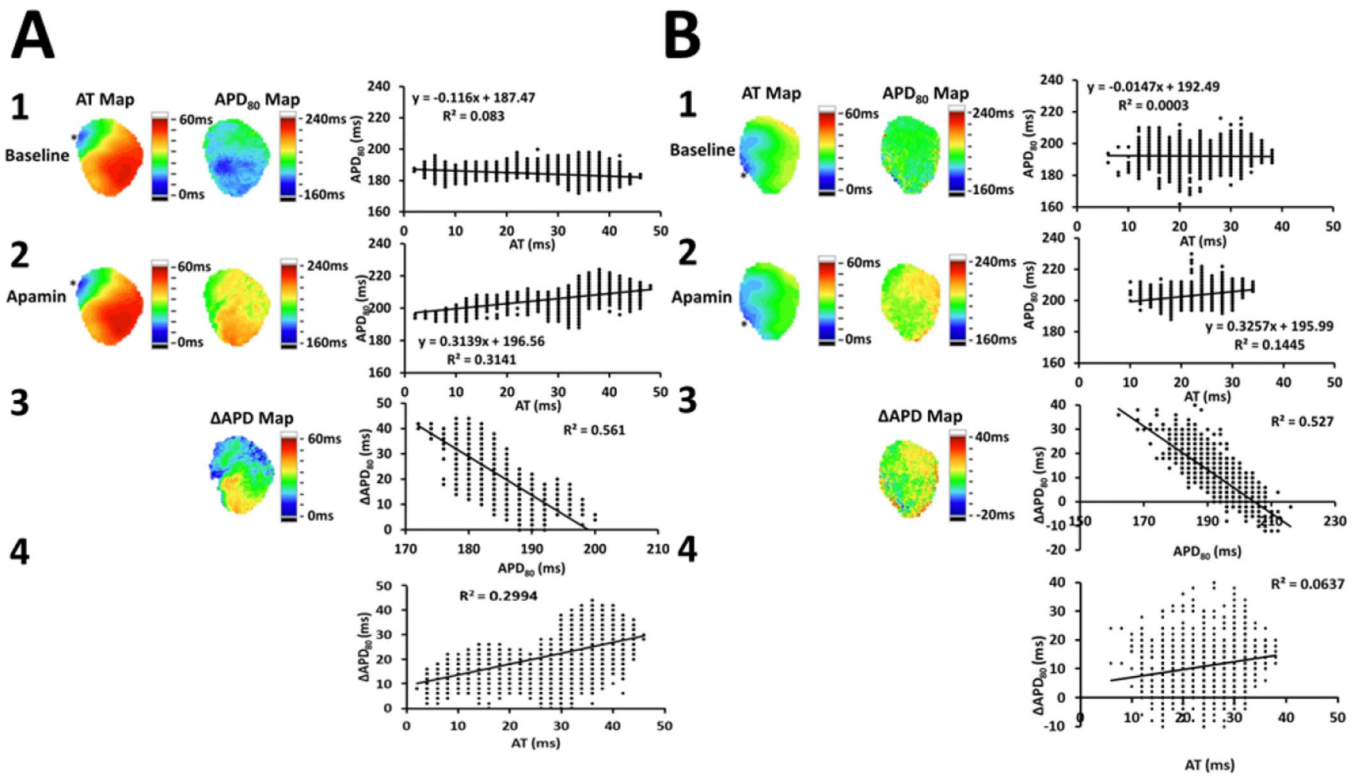

Figure 6.

Effects of I_{KAS} blockade on APD-to-AT relationship on the epicardium determined during RV pacing 300 ms PCL in hypokalemic ventricles. **A**, The AT maps, APD maps and corresponding plot of APD-AT relationship at baseline **(1)** and after apamin **(2)** infusion in one ventricle. The pacing site (asterisk) was located at RV base. Apamin increased the slope of APD-AT from −0.12 to 0.32. **(3)** The ΔAPD map and correlation between ΔAPD and baseline APD_{80} in the ventricle at PCL 300 ms. **(4)** The corresponding plot of ΔAPD-AT at PCL 300 ms. **B**, The AT maps, APD maps and corresponding pot of APD-AT relationship at baseline **(1)** and after apamin infusion **(2)** in another ventricle during 300 ms PCL. The pacing site is located at RV apex (asterisk). Apamin increased the slope of APD-AT from −0.01 to 0.33. **(3)** The ΔAPD map and correlation between ΔAPD and baseline APD_{80} in the ventricle at PCL 300 ms. **(4)** The corresponding plot of ΔAPD-AT at PCL 300 ms. APD = action potential duration; AT = activation time; I_{KAS} = apamin sensitive small conductance calcium activated potassium current; PCL = pacing cycle length; RV = right ventricle; ΔAPD = APD_{80} after apamin - APD_{80} at baseline.

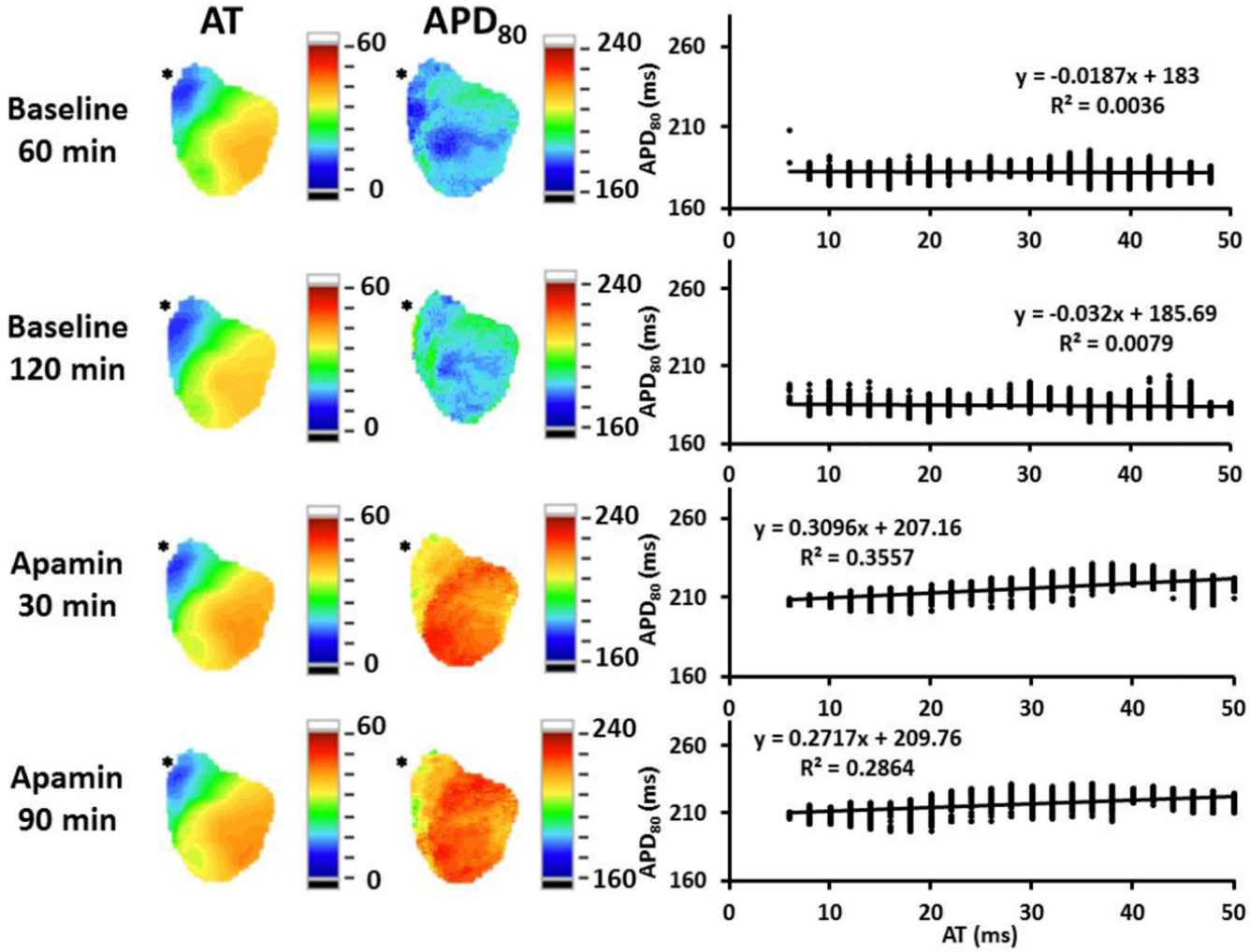

Figure 7.

APD-to-AT relationship over time. The rabbit ventricles were paced from the RV (asterisk) at 300 ms PCL. Maps were obtained at different times of the experiment as labeled on the left. The sequence of activation on the left ventricle was stable over time. The APD_{80}at baseline was stable for two hours. After addition of apamin, the $APD_{80}$was lengthened and the APD-to-AT slope increased at 30 min. These changes were stable one hour later. The pacing site (asterisk) is located at RV base.

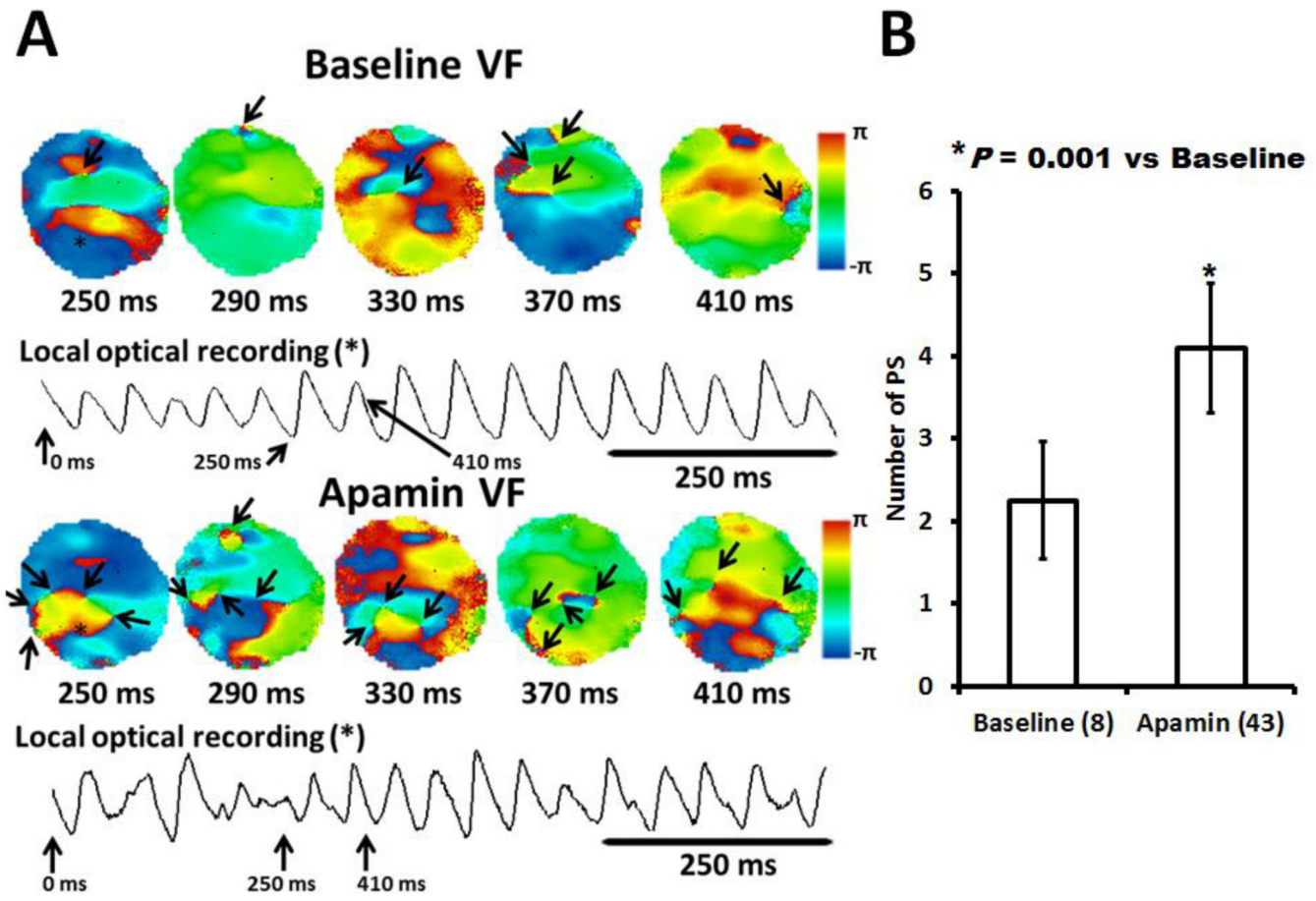

Figure 8.

Effects of I_{KAS} blockade on the wavebreaks of VF episodes in hypokalemic ventricles. **A**, Consecutive phase maps sampled at 40 ms during VF at baseline and after apamin infusion in one representative ventricle. Phase singularities (wavebreaks) are indicated by black arrows. The optical signals during VF came from a site marked by an asterisk. **B**, Effects of apamin on the number of phase singularities in all VF episodes before and after apamin infusion. Note that the phase singularities were significantly increased by apamin infusion. I_{KAS} = apamin sensitive small conductance calcium activated potassium current; PS, phase singularity; VF, ventricular fibrillation. *P = 0.001.